MAJOR ARTICLE

# *Plasmodium falciparum* Multidrug Resistance Protein 1 and Artemisinin-Based Combination Therapy in Africa

**Sabina Dahlström,[1,a] Pedro E. Ferreira,[1,5,a] M. Isabel Veiga,[1,5] Nazli Sedighi,[1] Lisa Wiklund,[1] Andreas Mårtensson,[1,3] Anna Färnert,[2] Christin Sisowath,[1] Lyda Osório,[6] Hamid Darban,[4] Björn Andersson,[4] Akira Kaneko,[1,7] Gwenaëlle Conseil,[8] Anders Björkman,[1] and J. Pedro Gil[1,2]**

[1]Malaria Research, and [2]Center of Molecular Medicine, Infectious Diseases Unit, Department of Medicine, [3]Division of Global Health, Department of Public Health Sciences, and [4]Institute Programme of Genomics and Bioinformatics, Department of Cell and Molecular Biology, Karolinska Institutet, Stockholm, Sweden; [5]Institute of Biotechnology and Bioengineering, Centre of Molecular and Structural Biomedicine, University of Algarve, Faro, Portugal; [6]Centro de Entrenimiento y Investigaciones Médicas, Cali, Colombia; [7]Global COE Program, Nagasaki University, Japan; [8]Division of Cancer Biology and Genetics, Cancer Research Institute, Queen's University, Kingston, Ontario, Canada

***Plasmodium falciparum*** **response mechanisms to the major artemisinin-based combination therapies (ACTs) are largely unknown. Multidrug-resistance protein (MRP)–like adenosine triphosphate (ATP)–binding cassette transporters are known to be related to multidrug resistance in many organisms. Therefore, we hypothesized that sequence variation in *pfmrp1* can contribute to decreased parasite sensitivity to ACT. Through sequencing of the *pfmrp1* open reading frame for 103 geographically diverse *P. falciparum* infections, we identified 27 single-nucleotide polymorphisms (SNPs), of which 21 were nonsynonymous and 6 synonymous. Analyses of clinical efficacy trials with artesunate-amodiaquine and artemether-lumefantrine detected a specific selection of the globally prevalent I876V SNP in recurrent infections after artemether-lumefantrine treatment. Additional in silico studies suggested an influence of variation in amino acid 876 on the ATP hydrolysis cycle of *pf*MRP1 with potential impact on protein functionality. Our data suggest for the first time, to our knowledge, the involvement of *pf*MRP1 in *P. falciparum* in vivo response to ACT.**

*Plasmodium falciparum* malaria remains a major public health problem. Recent findings, however, support the idea that new control strategies, including artemisinin-based combination therapy (ACT) and strengthened vector control, may provide a dramatic reduction in the burden of disease [1]. ACT has proven to be highly powerful for effective management of malaria, rapidly becoming a central tool for the control of the disease worldwide [2]. Development of resistance to ACT would have serious global public health consequences, similar to the failure of chloroquine as the mainstay antimalarial on the African continent during the 1980s and 1990s [3]. It is therefore critical to understand the mechanisms of ACT drug resistance at an early stage and find molecular markers that can be used as tools for monitoring the rise and spread of resistance. In this work, the possible involvement of multidrug-resistance

Received 30 January 2009; accepted 12 February 2009; electronically published 6 October 2009.

[a] S.D. and P.E.F. contributed equally to this work.

Reprints or correspondence: Sabina Dahlström, Malaria Research, Retzius väg 10 plan 5, 171 77 Stockholm, Sweden (sabina.dahlstrom@gmail.com).

**The Journal of Infectious Diseases 2009; 200:1456–64**

0022-1899/2009/20009-0014$15.00
DOI: 10.1086/606009

Potential conflicts of interest: none reported.

Presented in part: Federation of European Biochemical Societies (FEBS) Special Meeting ATP-Binding Cassette (ABC) Proteins: From Multidrug Resistance to Genetic Diseases, 4–10 March 2006, Innsbruck, Austria (poster 92); Molecular Approaches to Malaria, 3–7 February 2008, Lorne, Australia (poster 135); FEBS special meeting ATP-Binding Cassette (ABC) Proteins: From Multidrug Resistance to Genetic Diseases, 1–8 March 2008, Innsbruck, Austria (poster 89); Sweden-Japan Joint Seminar: Malaria Research—Diversity and Control, 11 June 2008, Stockholm, Sweden (oral presentation and poster abstract 27); Glutathione transferases, 20–24 August 2008, Uppsala, Sweden (poster).

Financial support: This work was supported by project grants from SIDA/SAREC SWE-2007-174 and SWE-2005-027, as well as from a nondisclosed Swiss foundation. P.E.F. and M.I.V. are recipients of PhD grants from Fundacão para a Ciência e Tecnologia/Ministerio da Ciência e Ensino Superior, Portugal—MCES (ref. SFRH/BD/28368/2006 and ref. SFRH/BD/28393/2006, respectively).

protein (MRP) homologues in the in vivo response to ACT was explored.

MRPs are members of the ATP-binding cassette (ABC) transporter superfamily [4]. These proteins are able to transport a large variety of substrates across membranes against a concentration gradient, in an energy-dependent reaction requiring ATP hydrolysis. Importantly, they transport xenobiotics and are thereby major contributors to drug resistance in a large range of organisms, including human tumor cells [5], bacteria [6], and parasites [7].

*P. falciparum* harbors 2 MRP homologues [8]. In this study, we focused on the *pfmrp1* gene, which codes for *pf*MRP1 (PFA0590w), an 1822–amino acid protein situated in the parasite plasma membrane [9]. Little was known about the possible role of MRPs in *P. falciparum* drug resistance. Previously, only an association of the *pfmrp1* SNPs Y191H and A437S with chloroquine and quinine in vitro sensitivity was reported [10], which could not be confirmed by others [11]. However, recent findings show that disruption of *pfmrp1* in the *P. falciparum* parasite W2 renders the parasite more sensitive to several antimalarial drugs, including chloroquine, quinine, and artemisinin. The *pfmrp1* knockout also accumulates more chloroquine and quinine, thus suggesting that *pf*MRP1 plays a role in parasite drug sensitivity through efflux of drugs [12].

Here we tested the hypothesis that an MRP protein contributes to the development of ACT resistance in vivo by examining the global biodiversity of the *pfmrp1* gene to identify new SNPs and furthermore by analyzing clinical isolates from 2 ACT efficacy trials conducted in East Africa before the implementation of these drugs. We searched for possible selection of *pfmrp1* SNPs after drug administration, as was done to establish *pfmdr1* polymorphisms as modulators of lumefantrine [13, 14] and amodiaquine [15] susceptibility in vivo. The combination therapies tested in the clinical trials were artesunate-amodiaquine (ASAQ) and artemether-lumefantrine (AL) (Coartem; Novartis), presently the major ACTs in wide-scale use in Africa. We also studied the impact of the main identified SNP on the protein structure in silico.

## MATERIALS AND METHODS

***Patients and culture-adapted* P. falciparum *parasites.*** The *pfmrp1* open reading frame (ORF) was sequenced for 103 *P. falciparum*–positive blood samples of different geographical origins. The samples were partly collected from travelers returning to Sweden with clinical malarial infections ($n = 35$) [16] after having visited Colombia (1), Suriname (1), Gambia (6), Guinea-Bissau (1), Guinea-Conakry (1), Liberia (2), Burkina Faso (1), Ghana (2), Togo (1), Benin (1), Nigeria (1), Cameroon (1), Namibia/Angola (1), Zimbabwe/Namibia (1), Zambia (1), Sudan (1), Malawi (1), Burundi (1), Central East Africa (1), Uganda (5), Kenya (1), Mozambique (1), Yemen (1), and Thailand (1). Additional patient samples originated from clinical studies conducted in Iran (4) [17], in Guinea-Bissau (5) [18], in Mali (2) [19], in Zanzibar (2) and at the Burma/Thailand border (13) and from malariometric surveys performed in Cambodia (15), Papua New Guinea (5), and Vanuatu (10). Finally, 12 culture-adapted *P. falciparum* parasite lines from Colombia with in vitro–determined median inhibitory concentration to amodiaquine and desethylamodiaquine [20] were also analyzed.

Samples from 2 clinical efficacy trials were included in an assessment of parasite polymorphisms and treatment outcome. The first trial, denoted ACO, was performed in Zanzibar from October 2002 through February 2003 and included 2 treatment arms comparing AL ($n = 200$) and ASAQ ($n = 208$) in children with uncomplicated malaria [21]. The second trial, herein named FUKA, was conducted from April through July 2004 in Fukayosi, Tanzania, and included 2 arms comparing AL ($n = 50$) and sulfadoxine-pyrimethamine ($n = 56$) [22]. Both studies had 42 days of follow-up after treatment. Blood was collected on filter papers at baseline and during follow-up. Because the intention was to assess the selection of SNPs upon ACT treatment, we analyzed all baseline infections but only the recurrent infections after ASAQ and AL treatment. The genetic region around amino acids 191 and 437 in *pf*MRP1 was sequenced in 70 samples from the ACO study and 30 from the FUKA study, because SNPs in these positions were previously identified in Kenya [23]. All blood samples analyzed in this report have been collected in studies that have been individually cleared by appropriate ethical authorities locally and/or in Sweden. All samples were obtained after receiving informed consent from the patients or their guardians.

***DNA extraction.*** Genomic DNA was extracted from whole blood or from blood spotted on filter paper by using the QIAamp DNA Blood Mini kit (Qiagen) or the ABI PRISM 6100 Nucleic Acid PrepStation (Applied Biosystems), according to methods described elsewhere [24].

***Sequencing of* pfmrp1 *ORF.*** The *pfmrp1* gene ORF was amplified by a long polymerase chain reaction (PCR) method modified from that of Sakihama et al [25]. The 5770-bp PCR product was used as a template for additional nested PCR amplifications. PCR and sequencing primers are described in Table 1. The obtained amplicons were sequenced by using the DYEnamic ET Dye Terminator Cycle Sequencing kit for MegaBACE DNA Analysis systems. The sequence reaction was followed by analysis on a MegaBACE 1000 devise (Amersham Bioscience).

**Table 1. Primers for *pf*MRP1 Polymerase Chain Reaction, Sequencing, and Pyrosequencing**

This table is available in its entirety in the online version of *Journal of Infectious Diseases*.

A minor part of the sequences were sent to Macrogen Inc. for sequencing.

***Pyrosequencing.*** The main identified SNPs in Africa, A2626G and A4397G (amino acid changes I876V and K1466R, respectively), in *pfmrp1* were analyzed by a pyrosequencing method modified from Dahlström et al [24] with the specific primers described in Table 1. A mixed genotype infection was defined as a pyrosequencing result between 10% and 90% for both genotypes, and a single-genotype (pure) infection was either above 90% or below 10%.

***Bioinformatic and statistical analyses.*** The *pf*MRP1 secondary structure was predicted with the HMMTOP algorithm (version 2). The *pf*MRP1 structure (Figure 1) was derived from hydropathy plots generated with the HMMTOP algorithm (version 2) [26, 27]. Sequencher software (versions 4.5 and 4.6) (Gene Codes Corporation) was used to analyze the sequences, with the 3D7 sequence of PFA0590w from PlasmoDB (http://plasmodb.org/) as the reference. The potential phenotypic consequences of the *pf*MRP1 SNPs were analyzed with the PolyPhen (http://genetics.bwh.harvard.edu.pph/) and SIFT (http://blocks.fhcrc.org/sift/SIFT.html) programs. The 2-tailed Fisher exact test was used to evaluate the difference in SNP prevalence between the baseline and recurrent infections. The $\chi^2$ test comparing observed and expected frequencies was used to test for an association between *pfmrp1* I876V and the previously analyzed *pfmdr1* N86Y and *pfcrt* K76T SNPs [13, 28]. Statistical calculations were performed with QuickCalcs software (GraphPad; http://graphpad.com/quickcalcs/).

***Structure and function analysis.*** To study the influence of the residue at amino acid position 876 on *pf*MRP1 functionality, we based our analysis on homologous regions of the crystalographically well-studied bacterial ABC transporter MsbA. Crystal structures trapped in different conformations were used from *Escherichia coli* (MsbA-EC) 3B5W (open apo), *Vibrio cholerae* (MsbA-VC) 3B5X (closed apo), and *Salmonella typhimurium* (MsbA-ST) in conformation with adenylyl-imidodiphosphate (AMPPNP), 3B60, or with adenosine diphosphate (ADP) vanadate, 3B5Z. Protein backbone and side-chain coordinates were generated by the MaxSprout tool at the European Bioinformatics Institute of the European Molecular Biology Laboratories [29]. Sequence analysis was performed with the Multialign server (http://mendel.ethz.ch:8080/Server/

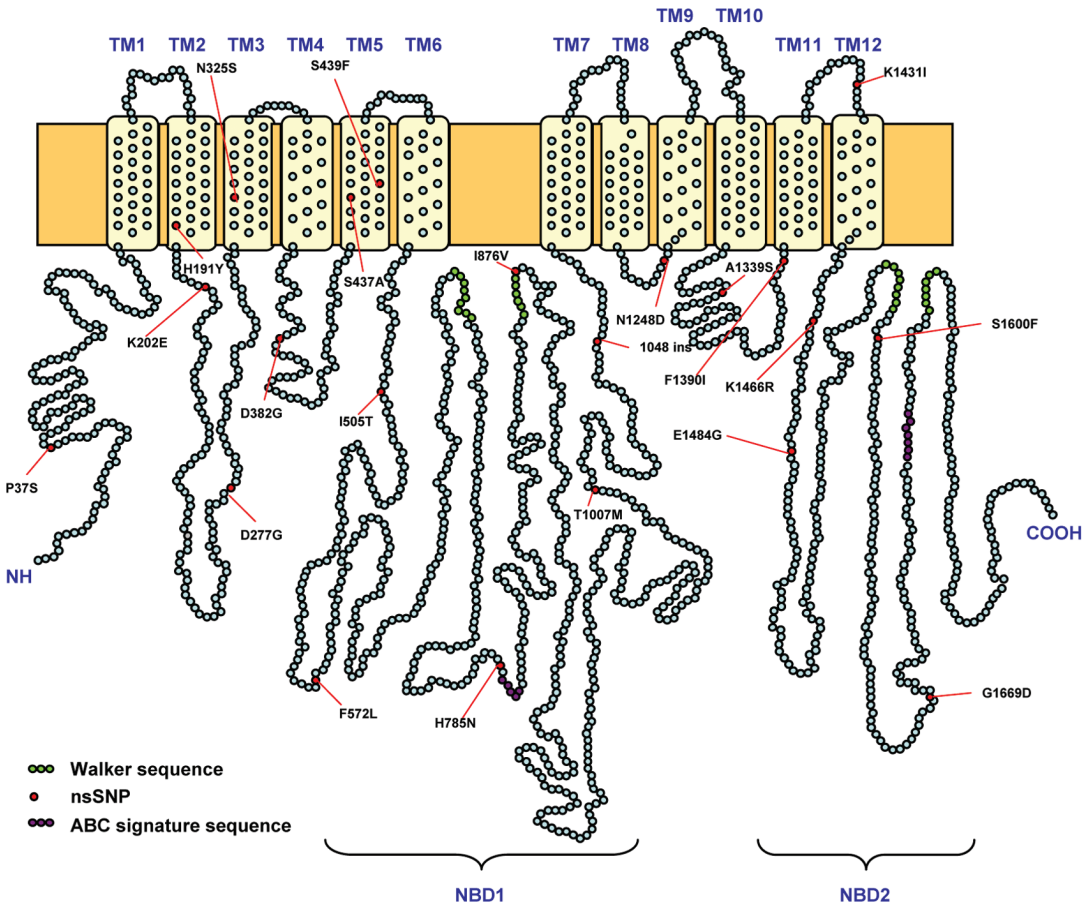


**Figure 1.** Predicted 2-dimensional transmembrane domain organization by the HMMTOP algorithm (version 2) and single-nucleotide polymorphism (SNP) distribution in *pf*MRP1. NBD, nucleotide binding domain; nsSNP, nonsynonymous SNP; TM, transmembrane domain.

**Table 2. Polymorphisms Identified in the *pf*MRP1 Gene by Sequencing and Their Geographical Source and Frequency**

| Nucleotide position | Triplet nucleotide change | Amino acid position | Amino acid change | Geographical source (proportion[a]) |
|---|---|---|---|---|
| 109 | CCG→TCG | 37 | P→S | PNG (3/5) |
| 300 | GCA→GCT | 100 | syn | Thailand (1/13) |
| 571 | CAT→TAT | 191 | H→Y | Iran (4/4), Thailand (12/14), Cambodia (13/15), PNG (4/5), Vanuatu (10/10) |
| 604 | AAA→GAA | 202 | K→E | PNG (3/5) |
| 830 | GAT→GGT | 277 | D→G | Mali (1/2) |
| 924 | ATT→ATC | 308 | syn | Zanzibar (1/66)[b] |
| 942 | CCG→CCC | 314 | syn | Ghana (1/2) |
| 974 | AAT→AGT | 325 | N→S | Thailand (2/14), Cambodia (3/15) |
| 1140 | TAT→TAC | 380 | syn | Thailand (1/14) |
| 1145 | GAT→GGT | 382 | D→G | Zanzibar (1/66)[b] |
| 1309 | TCA→GCA | 437 | S→A | Tanzania (1/28)[b], Zanzibar (1/66)[b], Iran (4/4), Thailand (11/13), Cambodia (11/13), PNG (4/5), Vanuatu (10/10) |
| 1316 | TCC→TTC | 439 | S→F | Zanzibar (1/66)[a] |
| 1514 | ATT→ACT | 505 | I→T | Zambia (1/1) |
| 1716 | TTC→TTG | 572 | F→L | Thailand (6/14), Cambodia (3/13) |
| 2353 | CAT→AAT | 785 | H→N | Thailand (7/13), Cambodia (7/14) |
| 2626 | ATA→GTA | 876 | I→V | Gambia (1/5), Malawi (1/1), Uganda (3/5), Kenya (1/1), Zanzibar (1/1), Iran (2/4), Thailand (11/13), Cambodia (10/13), PNG (4/5), Vanuatu (9/9) |
| 3020 | ACG→ATG | 1007 | T→M | Thailand (6/13), Cambodia (8/14) |
| 3144 | ins AATAAT | 1048 | ins NN | Namibia/Angola (1/1) |
| 3603 | GAA→GAG | 1201 | syn | Thailand (1/14) |
| 3742 | AAT→GAT | 1248 | N→D | Thailand (1/14) |
| 3999 | TCG→TCT | 1333 | syn | Thailand (1/14) |
| 4015 | GCA→TCA | 1339 | A→S | Iran (1/3) |
| 4168 | TTT→ATT | 1390 | F→I | Gambia (1/6), Iran (1/4), Thailand (5/14), Cambodia (2/15), PNG (3/5), Vanuatu (10/10) |
| 4292 | AAA→ATA | 1431 | K→I | Vanuatu (6/8) |
| 4397 | AAA→AGA | 1466 | K→R | Malawi (1/1), Guinea-Conakry (1/1), Ghana (1/2), Benin (1/1), Uganda (2/5), Kenya (1/1), PNG (2/3) |
| 4451 | GAA→GGA | 1484 | E→G | Thailand (1/14), Cambodia (1/13) |
| 4799 | TCT→TTT | 1600 | S→F | Thailand (1/13) |
| 5006 | GGT→GAT | 1669 | G→D | Thailand (1/14) |

**NOTE.** The 3D7 sequence of PFA0590w from PlasmoDB (http://plasmodb.org/) was used as the wild-type reference. ins, insertion; nucl., nucleotide; PNG, Papua New Guinea; syn, synonymous.

[a] No. of samples with pure plus mixed infection with the polymorphism per the total no. of successfully sequenced samples at the position.

[b] These samples were sequenced only around amino acid positions 191 and 437.

MultAlign.html), and the programs WinCoot (version 0.3.3) [30] and Yasara (version 8.11.11; http://www.yasara.org) were used for structural analysis. Using homology modeling, the *pf*MRP1 amino acid 876 was localized between the LSGGQ motif and the H loop in the nucleotide-binding domain (NBD). The 2 helices and the connecting loop in this region were analyzed for conformational changes, and different structures were superimposed with the Mustang algorithm [31]. ATP and $Mg^{2+}$ were located by superimposing the 3B60 structure on the cystic fibrosis transmembrane conductance regulator (CFTR) (1R10) structure (root mean square deviation, 1.185 Å). The I876V SNP was studied in a model generated for the *pf*MRP1 residues 867–894 segment that was based on the crystal structures of NBD sequence alignment in structure 3B60, using SCWRL2.8 [32] to make side-chain adjustments for the amino acid substitutions. DFprot software (http://sbg.cib.csic.ed/Software/DFprot/) [33] was used for flexibility and mobility analysis of primary sequences containing 876I or 876V.

## RESULTS

The several algorithms for hydropathy profile determination generally suggested that *pf*MRP1 is composed of a core domain of 12 transmembrane helices distributed in 2 membrane-spanning domains (MSDs), each followed by an NBD (Figure 1), confirming previous in silico analysis of the predicted coded protein [9].

The *pfmrp1* ORF was sequenced for 103 *P. falciparum* infections originating from most regions in which malaria is endemic (GenBank accession numbers FJ477732–FJ477834). More than 90% of the gene was successfully sequenced in 63 (61%) of 103 samples. The genetic regions around *pf*MRP1 amino acid

**Table 3. Frequencies of Genotypes at *pf*MRP1 Amino Acid Positions 876 and 1466 at Baseline and on Recurrent Days in the Artemisinin-Based Combination Therapy (ACT) Efficacy Trials**

| | 876 allele amino acid: no./total no., frequency | | 1466 allele amino acid: no./total no., frequency | |
|---|---|---|---|---|
| ACT (clinical trial) | Baseline[a] | Recurrent days | Baseline[a] | Recurrent days |
| ASAQ (ACO) | I: 309/402, 0.769 | I: 52/67, 0.776 | K: 178/369, 0.482 | K: 21/47, 0.447 |
| | V: 43/402, 0.107 | V: 8/67, 0.119 | R:51/369, 0.138 | R: 8/47, 0.172 |
| | I+V: 50/402, 0.124 | I+V: 7/67, 0.105 | K+R: 140/369, 0.379 | K+R: 18/47, 0.383 |
| AL (ACO) | I: 309/402, 0.769 | I: 35/38, 0.921[b] | K: 178/369, 0.482 | K: 18/31, 0.581 |
| | V: 43/402, 0.107 | V: 1/38, 0.026 | R:51/369, 0.138 | R: 8/31, 0.258 |
| | I+V: 50/402, 0.124 | I+V: 2/38, 0.053 | K+R: 140/369, 0.379 | K+R: 5/31, 0.161 |
| AL (FUKA) | I: 75/104, 0.721 | I: 33/38, 0.868 | K: 52/101, 0.515 | K: 23/37, 0.622 |
| | V: 13/104, 0.125 | V: 1/38, 0.026 | R: 25/101, 0.248 | R: 4/37, 0.108 |
| | I+V: 16/104, 0.154 | I+V: 4/38, 0.105 | K+R: 24/101, 0.238 | K+R: 10/37, 0.270 |
| AL (ACO+FUKA) | I: 384/506, 0.759 | I: 68/76, 0.895[b] | K: 230/470, 0.489 | K: 41/68, 0.603 |
| | V: 56/506, 0.111 | V: 2/76, 0.026 | R: 76/470, 0.162 | R: 12/68, 0.177 |
| | I+V: 66/506, 0.130 | I+V: 6/76, 0.079 | K+R: 164/470, 0.349 | K+R: 15/68, 0.221 |

**NOTE.** ACO and FUKA are the efficacy trials in Zanzibar and Tanzania, respectively. AL, artemether-lumefantrine; ASAQ, artesunate-amodiaquine; I, isoleucine; K, lysine; R, arginine; V, valine.

[a] The frequency prior to administration of drug (baseline) is based on samples from all of the patients enrolled in the study, independent of which treatment arm they were allocated to.

[b] The 2-tailed Fisher exact test ($P < .05$) was used to evaluate the difference in single-nucleotide polymorphism prevalence between the baseline and recurrent infections. Our statistical analyses were based on the pure selected genotype vs the unselected genotype together with the mixed genotypes.

positions 191 and 437 were successfully sequenced in 66 of 70 samples from Zanzibar (ACO) and 28 of 30 samples from mainland Tanzania (FUKA).

A total of 21 nonsynonymous and 6 synonymous SNPs were identified in *pfmrp1* (Table 2). An insert of 2 asparagines was also found in a region of asparagine repeats downstream of amino acid 1048, in 1 sample. The distribution of the identified SNPs suggests geographic region specific characteristics. Fourteen nonsynonymous SNPs were detected only in samples from Asia and Oceania, and no polymorphisms were observed in the South American samples. The previously identified SNPs at positions 191 and 437 were present at high frequencies in Asia and Oceania, whereas in Africa the H191Y SNP was not found and S437A was identified only in 2 samples with mixed alleles. The most common nonsynonymous SNPs in Africa were instead I876V and K1466R (Table 2). I876V was the most widely spread SNP, being present in Asian, African, and Oceanian parasite populations. This SNP is located in the predicted NBD1 of the protein, adjacent to the predicted Walker B motif (Figure 1).

When comparing the alterations in *pf*MRP1 identified here with the protein sequences of ABC transporters from *P. falciparum* and other parasites, I505T and T1007M were the only SNPs predicted by SIFT algorithms to potentially affect the function of *pf*MRP1. The I505T SNP was identified in only 1 sample from Zambia. The T1007M SNP was seen in 14 (52%) of 27 of the samples from Cambodia and Thailand. In contrast to the SIFT analysis, the PolyPhen analysis did not classify any of the SNPs as deleterious to the *pf*MRP1 function.

The main African SNPs— I876V and K1466R—were further analyzed in samples from the clinical trials ACO and FUKA. In ACO, there was a statistically significant positive selection of the pure 876I allele in the recurrent infections of the AL arm that was found in 35 (92.1%) of 38 recurrent infections compared to 309 (76.9%) of 402 baseline infections (2-tailed Fisher exact test, $P = .038$). Accordingly, the same tendency was observed in FUKA, with the pure 876I increasing from 75 (72.1%) of 104 at baseline to 33 (86.8%) of 38 in the AL recurrent infections (2-tailed Fisher exact test, $P = .079$). When pooling data from the 2 studies, a statistically significant selection of the pure 876I (75.9% vs 89.5%) (2-tailed Fisher exact test, $P = .007$) was observed after AL treatment (Table 3). There were no statistically significant changes in frequency of 876I in the ASAQ arm. No significant association was observed between I876V and the previously analyzed *pfmdr1* amino acid position 86 or *pfcrt* amino acid position 76, in either the ACO [13] or FUKA [28] trials. There were no statistically significant changes in the prevalence of the K1466R SNP in the AL arms or the ASAQ arm (Table 3).

Analysis of the different NBD crystal reference structures of the MsbA ABC transporter highlighted the conformational changes in the region between the LSGGQ motif and the H loop needed to create the binding pocket for ATP docking in the MsbA transporter. From the open-apo state to the ATP

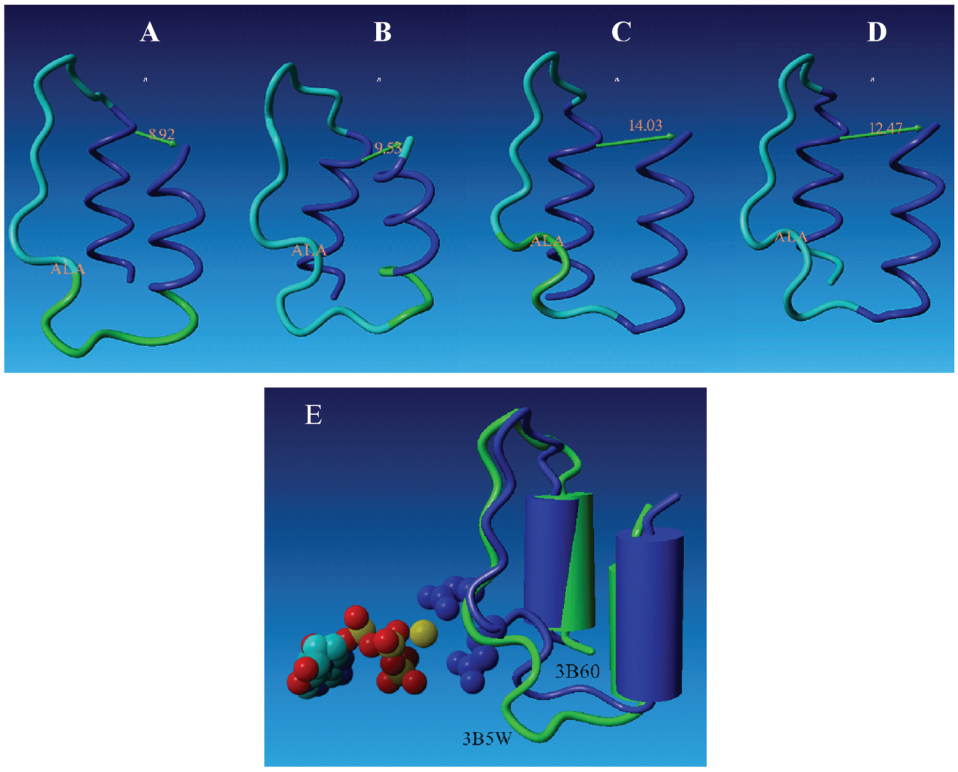


**Figure 2.** Mobility of the different nucleotide-binding domain (NBD) structures of MsbA, between the LSGGQ motif and the H loop. *A, Escherichia coli* (MsbA-EC) 3B5W (open apo). *B, Vibrio cholerae* (MsbA-VC) 3B5X (closed apo). *C, Salmonella typhimurium* (MsbA-ST) in conformation with adenylyl-imidodiphosphate (3B60). *D, Salmonella typhimurium* (MsbA-ST) in conformation with adenosine diphosphate (ADP) (3B5Z). Distances between helices appear in angstroms. Alanine denotes the amino acid homologous to 876 in *pf*MRP1. *E,* Superimposition of MsbA open-apo structure (*green*) and adenosine triphosphate (ATP) binding structure (*blue*). The yellow atom shows the magnesium bridge between side chains of the acidic residues (*blue*), homologous to residues 874 and 875 in *pf*MRP1, and the ATP molecule.

binding, we detected that helices between the LSGGQ motif and the H loop move apart, according to the measure of the distance between residues 495L and 525E (located in the different helices). Our analysis proposes a gradual increase in the distance between helices that follows the MsbA transporter functionality cycle: from the open-apo to the closed-apo state, there was a calculated increase from 8.92 to 9.53 Å in the distance (Figures 2*A*–2*B*). This was significantly increased to 14.03 Å when the transporter moved from the closed-apo state to nucleotide-binding state (Figure 2*C*). The distance between helices decreases when comparing the ATP-binding structure (14.03 Å) with the ADP-binding structure (12.47 Å) (Figure 2*D*), indicating a return to the transporter's open state and bringing the helices together and starting a new transport cycle. These events were followed by a conformational change in the connecting loop that twists and moves back toward the helices (Figure 2). The superimposition of the open apo and the nucleotide-binding structures summarizes the conformational changes needed for ATP docking and shows the mobility of the alanine residue corresponding to the 876 position in *pf*MRP1. Superimposition of the 3B60 struc-

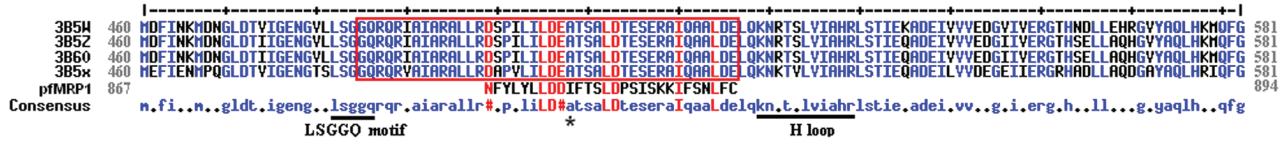


**Figure 3.** Alignment of MsbA protein sequences from crystal structures *Escherichia coli* (MsbA-EC) 3B5W (open apo), *Vibrio cholerae* (MsbA-VC) 3B5X (closed apo), and *Salmonella typhimurium* (MsbA-ST) in conformation with adenylyl-imidodiphosphate (3B60) and adenosine diphosphate vanadate (3B5Z). The red box shows the sequence of the structures of the MsbA transporters analyzed here. *pf*MRP1 sequence was modeled as shown in the alignment (see Figure 4). The asterisk (*) identifies position 876 in the *pf*MRP1 protein.

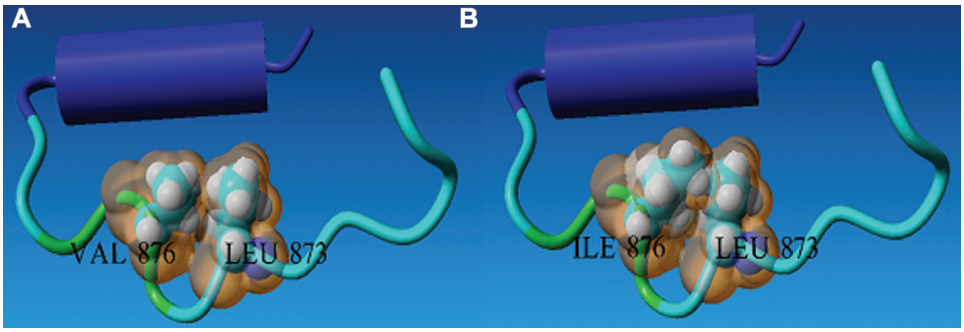


**Figure 4.** Side-chain contact between positions 876 and 873 in *pf*MRP1 protein. *A*, van der Waals radius of 876V side-chain contact with 873L. *B*, van der Waals radius of 876I side-chain contact with 873L.

ture in CFTR 1R10 indicates the importance of the acidic residues 505D and 506E, homologous to residues 874 and 875 in *pf*MRP1 (Figure 3), in ATP binding through the $Mg^{2+}$ bridge (Figure 2*E*).

To study the possible implications of the previous analysis for the *pf*MRP1 I876V polymorphism, we created a model of the protein region harboring the amino acid 876 position from the 3B60 MsbA homologous region (Figure 3). Since mobility and flexibility analysis using DFprot software showed no significant difference in the backbone structure characteristics (data not shown), we analyzed the side-chain contacts of amino acids 876I and 876V. The conformation of acidic residues 875 and 874 favors the approximation of the side chains of residues 876 and 873 (Figure 2*E*). The valine residue at position 876 created a contact in the van der Waals (VdW) surface with 873L residue (Figure 4*A*). The mass of residue valine is lower (99.132 g/mol) than isoleucine (113.159 g/mol), due to the presence of 1 more carbon in the side chain of isoleucine than in valine. This difference was reflected in the residue's radius, 4.213 Å for 876V and 4.652 Å for 876I. Accordingly, when valine was replaced by isoleucine in position 876, an overlap in VdW surface with residue 873 could be predicted (Figure 4*B*).

## DISCUSSION

*pf*MRP1 was observed to harbor significant biodiversity, with some of the identified SNPs showing geographical specificity, with generally less polymorphism observed in Africa, compared with that in Asia and Oceania (Table 2). Several SNPs are positioned near predicted functionally important protein regions (notably NBDs), suggesting the natural existence of coded *pf* MRP1 variants with variable transporting capacities. Among these SNPs, the I876V polymorphism stands out because of its close proximity to the NBD1/Walker B motif and its apparent global spread.

In the present study, the I876V polymorphism in *pfmrp1* was found to be under significant selection pressure after AL treatment, leading to the near disappearance of the valine-containing alleles. The majority of the AL recurrent infections in these studies represent new inoculations (reinfections) [21, 22]. Reinfecting parasites can be selected by subtherapeutic levels of the long half-life drug partner in ACT [34, 35]; selection of reinfections by lumefantrine after AL treatment has been previously reported [13, 14, 36, 37]. Therefore, we assume that the selection pressure effect observed here is derived mainly from selection of reinfections by subtherapeutic levels of lumefantrine. Conversely, no evidence of selection was observed after ASAQ treatment. This result was further supported by our analysis of culture-adapted parasites from Colombia that have no genetic variation in *pfmrp1*, despite widely variable responses to both amodiaquine (AQ) and its active metabolite desethylamodiaquine (DEAQ) [20].

*pf*MRP1 may influence the in vivo response to drugs via 2 non–mutually exclusive mechanisms: (1) by efflux of the drug, leading to a significant decrease in cytosol drug concentration and hence limiting its access to the target, and/or (2) by being an important contributor in the management of drug-driven oxidative stress, assuming that *pf*MRP1 represents a main oxidized glutathione (GSSG) efflux pump in *P. falciparum* [8], as observed in other biological systems [38].

The observed difference in the selection of genetic variation in *pfmrp1* could be explained by *pf*MRP1 being more important in the parasite response to lumefantrine than AQ. This could be due to either *pf*MRP1 substrate specificity, the location of the drug target, or the extent of the drug involvement in oxidative stress reactions. The variation itself could also change *pf*MRP1 drug specificity; however, this is less probable since this SNP is located in the NBD, which probably does not directly interact with the substrate. Many of these factors are unknown. However, the location of the drug targets could be different for the 2 drugs. Like chloroquine, another 4-aminoquinoline, the main AQ/DEAQ therapeutic target is likely to be located in the food vacuole. The target(s) of lumefantrine is not yet identified, but the drug could act outside the food vacuole, as proposed for both lumefantrine [28] and the related arylam-

inoalcohol, mefloquine [39]. Variation in plasma membrane efluxers such as *pf*MRP1 might then be of critical importance to the effect of lumefantrine, whereas variation in proteins located in the membrane of the food vacuole, such as *pf*CRT and Pgh-1, would better explain different in vitro responses to AQ or DEAQ [15, 20, 23].

The amino acid residue 876 is localized immediately downstream of the Walker B motif in NBD1 (Figure 1), a pivotal region in ATP binding and hydrolysis. To evaluate a possible functional influence of this polymorphism for ABC transporters' NBD functionality, we analyzed the structures of the MsbA transporter, a bacterial ABC transporter, in its different NBD conformations. The structures between the LSGGQ motif and the H loop, comprising the homologous region where the residue *pf*MRP1 876 localizes (Figure 3), were considered for conformational analysis. Our results suggest that this homologous region in the MsbA transporter is a dynamic zone of crucial importance for ATP binding. Mobility and flexibility analysis of the 876I and 876V backbone structure showed no significant changes in backbone characteristics, thus suggesting that differences in backbone conformations might not be the main reason for functional changes. We then analyzed the I876V side chains in 2 models, the main difference observed being a change in the residues 876/873VdW surface contact areas with the 876I variant overlapping with 873L. VdW forces are weak but are involved in numerous internal interactions between protein regions, being of significance for the final protein structure. In ABC transporters, protein mobility is the basis for protein functionality. This is well documented by Ward et al [40] regarding the transmembrane regions of the MsbA ABC transport. In the present work, we used the same approach [40] and focused on studying the NBD dynamics. We showed that NBD1 structures move to allow the binding of ATP to the essential acidic residues at the end of the Walker B motif. We postulate that nonpolar side chains between these residues play a role in stabilization of the pair of 2 acidic residues at the end of the Walker B motif, which is of major importance for $Mg^{2+}$ binding and consequent ATP docking to the NBD1. The VdW interaction could be of different kinds during 1 transport cycle (eg, attraction during ATP docking and repulsion after or during ATP hydrolysis) because of protein mobility and changes in the distance between its side chains. The latter would modulate the conformation of the acidic residue pair, influencing the binding of the $Mg^{2+}$ ions.

Because the cytosolic 876 amino acid position is most likely not located in a region of interaction with substrates, it is reasonable to ask what the drug-specific influence of this polymorphism could be. Our analysis showed that genetic variation in position 876 might affect the ATP-binding ability of the NBD of the protein. An altered activity of the ATP hydrolysis cycle is likely to affect the overall transport capacity of the protein, with the pharmacodynamic significance of this event being more visible with drugs specifically transported by *pf*MRP1. Assuming that *pf*MRP1 is not particularly associated with AQ/DEAQ response, variation in the NBD of this protein will not be of importance for this drug. On the other hand, variation in an amino acid of the NBD, such as at 876, could be expected to alter the rate of lumefantrine transport.

Although the precise molecular contribution of *pf*MRP1 for *P. falciparum* drug response remains unclear, our results indicate that its diversity is under lumefantrine selection pressure in vivo in a manner similar to the previously described selection of *pfmdr1* and *pfcrt* SNPs [13, 14, 28, 36]. Therefore, the influence of the herein-identified SNPs on parasite drug susceptibility merits further investigation. In conclusion, our data indicate that *pf*MRP1 may play an important role in future development of *P. falciparum* resistance to lumefantrine and, hence, to AL chemotherapy.

## Acknowledgments

We thank Prof Susan P. C. Cole (Queen's University, Kingston, Canada) for helpful discussions and valuable comments on the manuscript.

## References

1. Bhattarai A, Ali AS, Kachur SP, et al. Impact of artemisinin-based combination therapy and insecticide-treated nets on malaria burden in Zanzibar. PLoS Med **2007**; 4:e309.
2. Nosten F, White NJ. Artemisinin-based combination treatment of falciparum malaria. Am J Trop Med Hyg **2007**; 77:181–92.
3. Laufer MK, Djimde AA, Plowe CV. Monitoring and deterring drug-resistant malaria in the era of combination therapy. Am J Trop Med Hyg **2007**; 77:160–9.
4. Dassa E. Phylogenetic and functional classification of ABC (ATP-binding cassette) systems. In: Holland IB, Cole SPC, Kuchler K, Higgins CF, eds. ABC proteins from bacteria to man. London: Academic Press, **2003**; 3–36.
5. Haimeur A, Conseil G, Deeley RG, Cole SP. The MRP-related and BCRP/ABCG2 multidrug resistance proteins: biology, substrate specificity, and regulation. Curr Drug Metab **2004**; 5:21–53.
6. Poelarends GJ, Vigano C, Ruysschaert JM, Konings WN. Bacterial multidrug resistance mediated by ABC transporters. In: Holland IB, Cole SPC, Kuchler K, Higgins CF, eds. ABC proteins from bacteria to man. London: Academic Press, **2003**; 243–262.
7. Ouellette M, Légaré D. Drug Resistance mediated by ABC transporters in parasites of humans. In: Holland IB, Cole SPC, Kuchler K, Higgins CF, eds. ABC proteins from bacteria to man. London: Academic Press, **2003**; 317–34.
8. Bozdech Z, Ginsburg H. Antioxidant defense in *Plasmodium falciparum*: data mining of the transcriptome. Malar J **2004**; 3:23.
9. Klokouzas A, Tiffert T, van Schalkwyk D, et al. *Plasmodium falciparum* expresses a multidrug resistance-associated protein. Biochem Biophys Res Commun **2004**; 321:197–201.
10. Mu J, Ferdig MT, Feng X, et al. Multiple transporters associated with malaria parasite responses to chloroquine and quinine. Mol Microbiol **2003**; 49:977–89.
11. Anderson TJ, Nair S, Qin H, et al. Are transporter genes other than the chloroquine resistance locus (pfcrt) and multidrug resistance gene (pfmdr) associated with antimalarial drug resistance? Antimicrob Agents Chemother **2005**; 49:2180–8.

12. Raj DK, Mu J, Jiang H, et al. Disruption of a *Plasmodium falciparum* multidrug resistance-associated protein (PFMRP) alters its fitness and transport of antimalarial drugs and glutathione. J Biol Chem **2009**; 284: 7687–96.
13. Sisowath C, Stromberg J, Martensson A, et al. In vivo selection of *Plasmodium falciparum pfmdr*1 86N coding alleles by artemether-lumefantrine (Coartem). J Infect Dis **2005**; 191:1014–7.
14. Sisowath C, Ferreira PE, Bustamante LY, et al. The role of pfmdr1 in *Plasmodium falciparum* tolerance to artemether-lumefantrine in Africa. Trop Med Int Health **2007**; 12:736–42.
15. Holmgren G, Hamrin J, Svard J, Martensson A, Gil JP, Bjorkman A. Selection of pfmdr1 mutations after amodiaquine monotherapy and amodiaquine plus artemisinin combination therapy in East Africa. Infect Genet Evol **2007**; 7:562–9.
16. Farnert A, Tengstam K, Palme IB, et al. Polyclonal *Plasmodium falciparum* malaria in travelers and selection of antifolate mutations after proguanil prophylaxis. Am J Trop Med Hyg **2002**; 66:487–91.
17. Ursing J, Zakeri S, Gil JP, Bjorkman A. Quinoline resistance associated polymorphisms in the pfcrt, pfmdr1, and pfmrp genes of *Plasmodium falciparum* in Iran. Acta Trop **2006**; 97:352–6.
18. Ursing J, Kofoed PE, Rombo L, Gil JP. No *pfmdr*1 amplifications in samples from Guinea-Bissau and Liberia collected between 1981 and 2004. J Infect Dis **2006**; 194:716–8; author reply 718–9.
19. Bereczky S, Dolo A, Maiga B, et al. Spleen enlargement and genetic diversity of *Plasmodium falciparum* infection in two ethnic groups with different malaria susceptibility in Mali, West Africa. Trans R Soc Trop Med Hyg **2006**; 100:248–57.
20. Echeverry DF, Holmgren G, Murillo C, et al. Polymorphisms in the pfcrt and pfmdr1 genes of *Plasmodium falciparum* and in vitro susceptibility to amodiaquine and desethylamodiaquine. Am J Trop Med Hyg **2007**; 77:1034–8.
21. Martensson A, Stromberg J, Sisowath C, et al. Efficacy of artesunate plus amodiaquine versus that of artemether-lumefantrine for the treatment of uncomplicated childhood *Plasmodium falciparum* malaria in Zanzibar, Tanzania. Clin Infect Dis **2005**; 41:1079–86.
22. Martensson A, Ngasala B, Ursing J, et al. Influence of consecutive-day blood sampling on polymerase chain reaction–adjusted parasitological cure rates in an antimalarial-drug trial conducted in Tanzania. J Infect Dis **2007**; 195:597–601.
23. Holmgren G, Gil JP, Ferreira PM, Veiga MI, Obonyo CO, Bjorkman A. Amodiaquine resistant *Plasmodium falciparum* malaria in vivo is associated with selection of pfcrt 76T and pfmdr1 86Y. Infect Genet Evol **2006**; 6:309–14.
24. Dahlstrom S, Veiga MI, Ferreira P, et al. Diversity of the sarco/endoplasmic reticulum $Ca^{2+}$-ATPase orthologue of *Plasmodium falciparum* (PfATP6). Infect Genet Evol **2008**; 8:340–5.
25. Sakihama N, Mitamura T, Kaneko A, Horii T, Tanabe K. Long PCR amplification of *Plasmodium falciparum* DNA extracted from filter paper blots. Exp Parasitol **2001**; 97:50–4.
26. Tusnady GE, Simon I. Principles governing amino acid composition of integral membrane proteins: application to topology prediction. J Mol Biol **1998**; 283:489–506.
27. Tusnady GE, Simon I. The HMMTOP transmembrane topology prediction server. Bioinformatics **2001**; 17:849–50.
28. Sisowath C, Petersen I, Veiga MI, et al. In vivo selection of *P. falciparum* parasites carrying the chloroquine-sensitive *pfcrt* K76 allele upon treatment with artemether-lumefantrine in Africa. J Infect Dis **2009**; 199: 750–7.
29. Labarga A, Valentin F, Anderson M, Lopez R. Web services at the European bioinformatics institute. Nucleic Acids Res **2007**; 35:W6–11.
30. Emsley P, Cowtan K. Coot: model-building tools for molecular graphics. Acta Crystallogr D Biol Crystallogr **2004**; 60:2126–32.
31. Konagurthu AS, Whisstock JC, Stuckey PJ, Lesk AM. MUSTANG: a multiple structural alignment algorithm. Proteins **2006**; 64:559–74.
32. Bower MJ, Cohen FE, Dunbrack RL Jr. Prediction of protein side-chain rotamers from a backbone-dependent rotamer library: a new homology modeling tool. J Mol Biol **1997**; 267:1268–82.
33. Kovacs JA, Chacon P, Abagyan R. Predictions of protein flexibility: first-order measures. Proteins **2004**; 56:661–8.
34. White N. Antimalarial drug resistance and combination chemotherapy. Philos Trans R Soc London B Biol Sci **1999**; 354:739–49.
35. Stepniewska K, White NJ. Pharmacokinetic determinants of the window of selection for antimalarial drug resistance. Antimicrob Agents Chemother **2008**; 52:1589–96.
36. Dokomajilar C, Nsobya SL, Greenhouse B, Rosenthal PJ, Dorsey G. Selection of *Plasmodium falciparum* pfmdr1 alleles following therapy with artemether-lumefantrine in an area of Uganda where malaria is highly endemic. Antimicrob Agents Chemother **2006**; 50:1893–5.
37. Happi CT, Gbotosho GO, Folarin OA, et al. Selection of *Plasmodium falciparum* multidrug resistance gene 1 alleles in asexual stages and gametocytes by artemether-lumefantrine in Nigerian children with uncomplicated falciparum malaria. Antimicrob Agents Chemother **2009**; 53:883–95.
38. Leier I, Jedlitschky G, Buchholz U, et al. ATP-dependent glutathione disulphide transport mediated by the MRP gene-encoded conjugate export pump. Biochem J **1996**; 314:433–7.
39. Famin O, Ginsburg H. Differential effects of 4-aminoquinoline-containing antimalarial drugs on hemoglobin digestion in *Plasmodium falciparum*-infected erythrocytes. Biochem Pharmacol **2002**; 63:393–8.
40. Ward A, Reyes CL, Yu J, Roth CB, Chang G. Flexibility in the ABC transporter MsbA: alternating access with a twist. Proc Natl Acad Sci U S A **2007**; 104:19005–10.